Kinetics of the $O(^3P) + N_2O$ Reaction. 1. Direct Measurements at Intermediate Temperatures

Arthur Fontijn,* Abdellatif Goumri,† and Abel Fernandez

High-Temperature Reaction Kinetics Laboratory, The Isermann Department of Chemical Engineering, Rensselaer Polytechnic Institute, Troy, New York 12180-3590

William R. Anderson* and Nancy E. Meagher‡

U.S. Army Research Laboratory, Aberdeen Proving Grounds, Maryland 21005-5066

Received: December 23, 1999

Rate coefficients for the consumption of O atoms by their reaction with N_2O have been measured, at pressures from 130 to 500 mbar, using the high-temperature photochemistry technique. These represent the first direct measurements of k values of the reaction. The ground-state oxygen atoms were produced by laser photolysis of SO_2, or by flash photolysis of either SO_2 or O_2, and monitored by time-resolved resonance fluorescence. The results yield $k(1075-1140\ \mathrm{K}) = 3.2 \times 10^{-11} \exp(-9686K/T)\ \mathrm{cm^3\ molecule^{-1}\ s^{-1}}$ with 2σ precision limits of ±12% and corresponding 2σ accuracy limits of ±26%. Results from several sources in the literature indicate a high sensitivity of the $O + N_2O$ reaction system to traces of H_2O, which increases the rates if present as a contaminant. For this reason, possible effects of traces of H_2O on the results were modeled. Simulated decay curves with a hypothetical H_2O contaminant were used as a test of the experimental data reduction procedures. Although the concentration of H_2O needed to significantly affect the results is small, the amount that could have been present is even less and is shown to have had negligible effects. The results are in qualitative agreement with a recent $T \geq 1680$ K shock tube study (D. F. Davidson, M. D. DiRosa, A. Y. Chang, and R. K. Hanson, ref 9) in that extrapolation of their results to the present temperatures indicates rate coefficients much larger than had been previously thought. However, though the results agree within error limits for such a long extrapolation, the present results are about a factor of 4 smaller. Combined with the results of the companion paper by Meagher and Anderson (ref 6, following paper in this issue), in which the prior literature is critically reevaluated, it is found that the $O_2 + N_2$ product channel dominates at the present temperatures.

I. Introduction

The role of nitrous oxide (N_2O) in combustion and its thermal decomposition have been studied extensively. Motivation for the present investigation stems from the fact that N_2O is a major intermediate oxidizer species formed during the combustion of many types of solid propellants and their energetic raw materials.[1] Therefore, it is important for the development of solid propellant models to understand the role of this oxidizer in the combustion process. N_2O also plays a major role in the formation of NO_x pollutants during combustion.[2] In addition, dissociation of nitrous oxide offers the possibility of initiating combustion reactions by the atomic oxygen produced,[3] and has been used as a test case for unimolecular reaction theories.[4]

For the preceding reasons, it is important to understand the reactions of N_2O with the three primary combustion radicals, H, O, and OH. The reaction of N_2O with O atoms, which plays major roles in both the combustion and the thermal decomposition of N_2O, has two significant product channels:

$$O + N_2O \rightarrow NO + NO \qquad \Delta H_0 = -36\ \mathrm{kcal/mol}\ \text{(R1)}$$

$$O + N_2O \rightarrow O_2 + N_2 \qquad \Delta H_0 = -79\ \mathrm{kcal/mol}\ \text{(R2)}$$

An early critical review[5] (BDH73) of the extensive literature published through 1973 on $O + N_2O$ and other reactions concluded that the two channels have identical rate coefficients:

$$k_1(\mathrm{T}) = k_2(\mathrm{T}) = 1.7 \times 10^{-10} \exp(-14100K/T)\ \mathrm{cm^3\ molecule^{-1}\ s^{-1}}\ (1200-2000\ \mathrm{K}) \quad (1)$$

Modeling of some of the experiments utilized to determine the k_1 recommendation of BDH73 has recently been performed. This work is discussed in detail in the following paper in this issue.[6] The study has revealed that assumptions about the ancillary chemistry utilized in complex modeling to extract k_1, or its reverse, from the data in some of the most important of the works cited in BDH73 are incorrect, invalidating both those results and the BDH73 recommendation. It is also shown in ref 6 that at temperatures below about 1700 K most of the currently available studies for k_1 and all for k_2 are invalid. The k_1 expression from BDH73 strongly affects most of the later recommendations. Subsequent reviews have accepted the soundness of the choices made in BDH73 regarding the best values from early works. The expression given in eq 1 was used as

† Current address: Department of Chemistry, University of North Texas, Denton, TX 76203.

‡ Contribution performed in part as an ASEE Postdoctoral Research Associate at the U.S. Army Research Laboratory. Current address: Department of Chemistry and Physics, Texas Woman's University, Denton, TX 76204.

10.1021/jp994470v CCC: $19.00
Published on Web 06/02/2000

part of the fitted data to obtain a k_1 recommendation in ref 7 (HS85). Recommendations from HS85 for the two channels are

$$k_1(\mathrm{T}) = 1.2 \times 10^{-10} \exp(-13400K/T)\ \mathrm{cm^3\ molecule^{-1}\ s^{-1}} \quad (1200-4100\ \mathrm{K}) \quad (2)$$

$$k_2(\mathrm{T}) = 1.7 \times 10^{-10} \exp(-14100K/T)\ \mathrm{cm^3\ molecule^{-1}\ s^{-1}} \quad (1200-3200\ \mathrm{K}) \quad (3)$$

These expressions only differ modestly from those of BDH73. The recommendations of HS85 were subsequently accepted in a review pertinent to propellant chemistry modeling.[8] However, a recent high-temperature shock tube determination[9] (DDCH92), which involved direct UV absorption measurements of the O_2 and NO products, yielded a very different result:

$$k_1(\mathrm{T}) = 4.8 \times 10^{-11} \exp(-11650K/T)\ \mathrm{cm^3\ molecule^{-1}\ s^{-1}} \quad (1680-2430\ \mathrm{K}) \quad (4)$$

$$k_2(\mathrm{T}) = 2.3 \times 10^{-12} \exp(-5440K/T)\ \mathrm{cm^3\ molecule^{-1}\ s^{-1}} \quad (1940-3340\ \mathrm{K}) \quad (5)$$

k_1 from DDCH92 agrees very well with that from HS85. But, although the magnitude of k_2 is similar to that of previous expressions at ~2000 K, the slope of the Arrhenius plot is very different. The activation energy, E_a, corresponding to k_2 is only 11 kcal/mol as opposed to ~28 kcal/mol from prior sources. Thus, extrapolation of the k_2 expression to lower temperatures, where few data are available, would lead to much larger total rate coefficients than yielded by the earlier expressions. The two sets of expressions from HS85 and DDCH92 were recently tested by comparison of flow system data on $CO/N_2O/H_2O/N_2$ mixtures at 950−1123 K vs modeling results using a complex mechanism.[10] That work concludes that the data favor adoption of expressions from HS85 rather than DDCH92. However, rate coefficients of magnitude between those of HS85 and DDCH92 were not tested. The expressions from DDCH92 are recommended in a recent critical review[11] with an admonition that there is still "appreciable uncertainty" regarding k_2.

The $O + N_2O$ reaction is important at all temperatures for propellant chemistry. Temperatures between 1200 and 1600 K are especially pertinent to modeling the dark zone structure of solid propellants (nonluminous gaseous region between the condensed-phase propellant and luminous flame zone[1a]). The uncertainty regarding the extrapolation to lower temperatures and the lack of any prior measurements under isolated conditions indicated a need for a direct determination of the reaction rate coefficients at temperatures below 1700 K. The analysis errors in prior works indicated a need for a thorough reassessment of the literature regarding this reaction. Note in this and the companion paper,[6] "intermediate temperatures" refer to the approximate range 1000−1700 K and "high temperatures" to higher values.

The first measurements of the title reaction under conditions in which it is clearly isolated from the effects of other reactions (that is, complex modeling with heavy reliance on ancillary kinetic data is *not* required to extract the rate coefficients) are reported in this paper. Measurements of the total rate of O atom disappearance in an excess of known concentrations of N_2O were performed at the Rensselaer Polytechnic Institute (RPI) using the HTP (high-temperature photochemistry) technique. Modeling of the possible effects of H_2O as a contaminant, whose effects have been suggested in another recent N_2O study,[12] was done at the U.S. Army Research Laboratory. The modeling provides an estimate of the concentrations of H_2O necessary to significantly affect the results. Although the necessary amounts are very small, the effects of H_2O are proven to be insignificant. Results have been obtained for the total reaction rate coefficients, $k_{tot} = k_1 + k_2$, in the temperature range 1076−1276 K.

In the companion paper,[6] an evaluation of all literature relevant to the title reaction and new recommendations for k_1 and k_2 are presented, utilizing all retained data to provide fits. The present experimental results are that k_{tot} is indeed much larger at intermediate temperatures than had been previously believed, but not as large as extrapolation of DDCH92 would suggest.

II. Experimental Procedures

The older style HTP reactor[13] was used. Briefly, it consists of an alumina reaction tube (5.1 cm i.d.) which is surrounded by helical SiC heating elements and insulation and enclosed in a water-cooled, steel vacuum chamber. To achieve the desired temperatures without decomposition of the reactant gases, a movable, air-cooled inlet is used. After emerging, the gases are mixed with the heated Ar bath gas. The residence time needed for the mixture to reach the reaction zone is adjusted so that the reactant gases are at least 95% mixed with Ar.[14] The temperature of the reaction zone was measured before and after each experiment by a Pt−Pt/13% Rh thermocouple, which was doubly shielded to minimize radiation effects. An FPI pressure transducer was used. The gas flow rates were controlled by Teledyne-Hasting flow controllers.

Ground-state $O(^3P)$ atoms were generated by laser photolysis of SO_2 at 193 nm or by flash photolysis of either SO_2 (through a Suprasil Quartz window) or O_2 (through a MgF_2 window). The decrease in the relative concentration of $O(^3P)$ atoms was monitored by fluorescence of the 130.2−130.6 nm resonance triplet. The fluorescence was induced by a cw microwave discharge lamp, through which flowed 99.999% He which contains O_2 as an impurity. A CaF_2 lens was used to focus the O atom radiation and filter Lyman α-radiation. The O atom fluorescence was detected by a solar blind photomultiplier tube (PMT) and fed to a multichannel scaler signal averager.

The experiments were carried out under pseudo-first-order conditions, where $[O] \ll [N_2O] \ll [Ar]$. Under these conditions, the fluorescence intensity I, which is proportional to [O], is expressed by

$$I = I_o \exp(-k_{ps1}t) + B \quad (6)$$

where $k_{ps1} = k_{tot}[N_2O]$ is the pseudo-first-order rate coefficient, $I_o + B$ the intensity at time $t = 0$, and B the background, due mainly to scattered light. The values of k_{ps1} were obtained by a weighted fit of the observed I vs t profiles to eq 6.[15] Typically, five or six k_{ps1} measurements at varying $[N_2O]$, with the minimum $[N_2O]$ a factor of about 5−10 lower than the maximum values listed in Table 1, were used to obtain k_{tot} at the temperature and pressure of the experiment.

The exponentiality of the I vs t plots was tested by a two-stage residual plot analysis consisting of, first, a visual inspection of the plotted residuals (experimental minus fitted values) and, second, a runs test.[16] The data must pass both tests. An example of an experimental [O] decay, its fit to eq 6, and the associated residuals plot are given in Figure 1. The residuals consist of both positive and negative values. In Figure 1, these occur in a band centered about zero; thus, that decay passes the visual inspection test. For a given decay, the runs test gives a measure of how "random" the residuals are by comparing the actual number of runs (the number of groups of adjacent residuals

TABLE 1: Summary of Rate Coefficient Measurements on the $O + N_2O$ Reaction

T[a] (K)	P (mbar)	[M] (10^{18} cm^{-3})	[photolyte] (10^{14} cm^{-3})	F (mJ)	$[N_2O]_{max}$ (10^{15} cm^{-3})	z (cm)	$\bar{v}$ (cm s^{-1})	$k_i \pm \sigma_{k_i}$ (10^{-14} cm^3 molecule^{-1} s^{-1})
1076	413	2.78	1.72	40	4.00	17	12	0.36 ± 0.02
1076	492	3.31	4.84	27	3.00	10	7	0.45 ± 0.01
1097	375	2.47	2.35	33	4.30	10	9	0.45 ± 0.04
1099	283	1.87	1.60	40	3.70	10	14	0.40 ± 0.01
1101	197	1.30	1.59[c]	13[d]	3.42	8	14	0.48 ± 0.06
1121	228	1.47	9.60[b]	22[d]	2.90	8	11	0.55 ± 0.03
1132	320	2.04	5.01	40	3.12	10	13	0.71 ± 0.06
1141	355	2.24	7.94[c]	50[d]	4.50	8	6	0.62 ± 0.14
1142	133	0.84	2.50[c]	13[d]	3.10	10	16	0.75 ± 0.06
1142	324	2.05	3.24[c]	22[d]	4.32	10	8	0.53 ± 0.07
1178	496	3.05	4.15	40	4.40	10	7	1.12 ± 0.12
1178	549	3.45	4.70	27	4.50	16	7	1.01 ± 0.08
1179	495	3.10	2.58	13	3.40	5	9	1.55 ± 0.14
1179	556	3.40	4.85	53	4.00	10	8	1.57 ± 0.11
1202	148	0.89	3.66[c]	50[d]	2.11	10	16	1.40 ± 0.15
1219	328	1.95	9.80[c]	22[d]	2.50	17	9	1.29 ± 0.07
1230	475	2.80	5.50	47	5.80	10	8	2.02 ± 0.20
1230	526	3.14	6.12	13	7.10	10	7	1.38 ± 0.06
1251	176	1.00	8.00[b]	9[d]	2.40	8	14	2.61 ± 0.14
1272	400	2.30	2.80	20	4.07	10	10	3.06 ± 0.13
1273	345	1.97	4.1	40	4.72	10	10	2.96 ± 0.12
1276	403	2.28	2.52	33	4.48	6	10	3.02 ± 0.18

[a] $\sigma_T/T = \pm 2\%$. [b] O_2 was photolyzed by the flash lamp through a MgF_2 window. [c] SO_2 was photolyzed by the flash lamp through a Suprasil window. [d] For these flash-lamp experiments these energies are in joules; all of the other experiments used laser photolysis of SO_2, with energies expressed in millijoules.

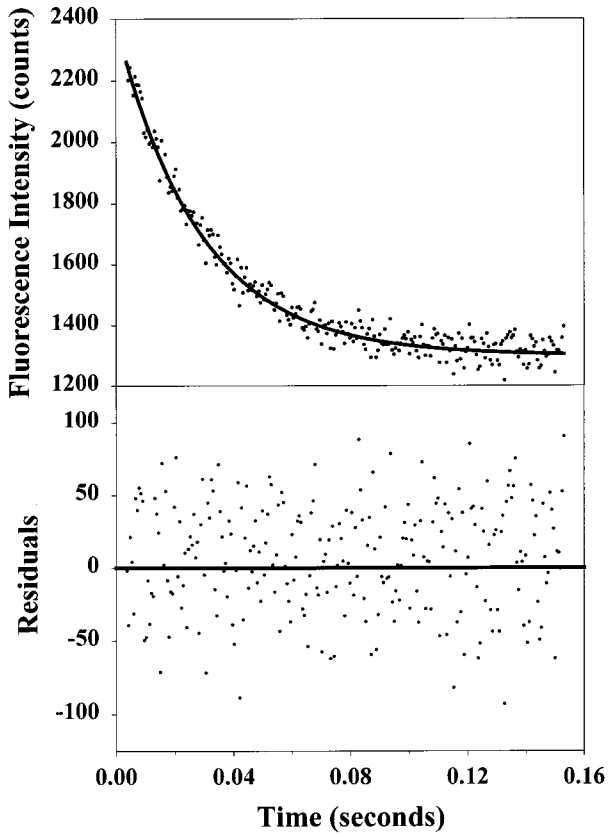

Figure 1. Example experimental [O] decay and residuals plot at 1142 K, total pressure 133 mbar, and $[N_2O] = 1.1 \times 10^{15}$ cm^{-3}. The fitted I_o, k_{ps1}, and B values are 1088.7, 34.67 s^{-1}, and 1300, respectively. $Z = -0.014$. Contribution to k_{ps1} due to diffusion found by fitting the ($[N_2O]$, k_{ps1}) data, $k_d = 26$ s^{-1}. Upper panel: measured decay (points) and fit to eq 6 (curve). Lower panel: residuals plot; a line is drawn at zero in the lower panel as an aid for visual inspection.

having the same sign), u, to the mean number of such runs expected for the number of data points used in the fit. Assuming that the number of runs follows a normal distribution, the deviation of u from the mean is given by the unit normal deviate, Z.[16,17] Z gives a quantitative measure to decide whether the residuals are randomly distributed about the fitted curve. We have found that a stringent and adequate criterion is $|Z| \leq 1.5$; this corresponds to a rejection region in the 6.68% tails of the normal distribution.

The possible effects of contaminants, especially H_2O, on the N_2O system reactions are of considerable concern. Normal precautions in performing the experiments are described below to emphasize the validity of the data presented herein. All supply lines leading to the reactor are kept at pressures above atmospheric up to the flow controllers which are in line just prior to the reactor. All parts of the apparatus, especially the flow lines at subatmospheric pressure, were regularly checked with a helium leak detector. The reactor, as a matter of course, is continuously baked out at high temperature; thus, it cannot be a source of significant H_2O. Therefore, there are two major contaminant sources to consider, the supply gases and air leaks. Only high-purity gases were used (see below). It is only important to consider the Ar carrier gas since the others are present in much smaller amounts and were passed through drying towers. The carrier could have up to 20 ppm impurity. However, the carrier is stored as a liquid and vaporized as needed during the experiments. Thus, any impurities in the carrier must have a very low boiling point to pass into the test mixture. H_2O from this source is clearly excluded. Air leaks would lead to addition of, mainly, N_2, O_2, Ar, and H_2O to the test mixture. The first three would have no effect on the present experiments. Since the modeling indicates a very high sensitivity to H_2O as a contaminant, a measurement of the air leak rate was performed at operating temperatures. From this, it was inferred that the maximum concentration of H_2O which could possibly be present in the reactor is 0.2 ppm, assuming a laboratory relative humidity of 100%.

The gases used were N_2O (99.99%) from Matheson, 5% O_2 (99.99%) in Ar (99.998%) from Scott, 1% SO_2 (99.98%) in Ar (99.998%) from Matheson, and Ar (99.998%) from the liquid (Praxair).

TABLE 2: Subset of Important Reactions Extracted from the Detailed Mechanism Used for Modeling the Effects of Hypothetical H_2O Contaminant[a]

no.	reaction		A	n	E_a/R	ref
R1	$O + N_2O \rightarrow NO + NO$			see the text		
R2	$O + N_2O \rightarrow O_2 + N_2$			see the text		
R3	N_2O (+M) $\rightarrow N_2 + O$ (+M)	k_0	9.91E−10	0.00	28 510	21
		k_∞	1.26E+12	0.00	31 510	
	efficiencies, η_i: /Ar 0.67/N_2O 5.0/ from ref 5 /H_2O 7.5/O_2 0.82/ from ref 22					
R4	$H + N_2O \rightarrow N_2 + OH$		3.70E−10	0.00	8 430[b]	14
			4.20E−14	0.00	2 290[b]	
R5	$H + O_2 \rightarrow O + OH$		5.85E−08	−0.70	8 590	23
R6	$OH + OH \rightarrow O + H_2O$		9.96E−16	1.30	0	2
R7	NO_2 (+M) $\rightarrow NO + O$ (+M)	k_0	4.10E+04	−3.37	37 640	8
		k_∞	7.60E+18	−1.27	36 880	
	efficiencies, η_i: /Ar 0.71/N_2O 1.5/H_2O 4.4/ from ref 5, reverse reaction					
R8	$NO_2 + O \rightarrow NO + O_2$		6.48E−12	0.00	−120	8

[a] Units are cm^3, molecule, s, K. The parameters A, n, and E_a/R are for rate coefficient expressions in the form $k = AT^n \exp(-E_a/RT)$. For the falloff reactions, R3 and R7, the overall collider efficiencies are given by $C_M = [P/RT]\sum_{i=1}^{N} X_i\eta_i$, where P is pressure and X_i and η_i are the mole fraction and the collider efficiency, respectively, of species i. The expressions are appropriate for an N_2 collider efficiency of 1.0, adjustments to low pressure A factors having been made where necessary. Rate coefficients of the reactions are then given using $k = Fk_\infty k_L$, where $k_L = k_0C_M/(k_\infty + k_0C_M)$ and $\log F = \log F_C/\{1 + [\log (k_0C_M/k_\infty)]^2\}$. For reaction R3, the simple Lindemann form, $F = 1.0$, is used.[21] For reaction R7, $F_C = 0.95-1.0 \times 10^{-4}$ T is used.[8] [b] For reaction R4, the rate coefficient is computed as the sum of the two exponential expressions.

III. Consideration of H_2O as Hypothetical Contaminant

As previously mentioned, the authors of ref 12 have shown that the thermal decomposition of N_2O can be substantially accelerated by traces of H_2O, even at temperatures above 1700 K. Further discussions about its pronounced effect at lower temperatures are presented in ref 18, which contains calculations for a presumed 30 ppm H_2O as contaminant, and in ref 19, a combined experimental flow reactor/modeling study in which H_2O was deliberately added at a known concentration of 560 ppm. The prior observations of strong effects of H_2O, and the fact that the present results for k_{tot} are much larger than had previously been believed,[5,7,8] raised concerns about the sensitivity of the present experimental results to the presence of trace amounts of H_2O. For this reason, the experiments were modeled using a state-of-the-art detailed chemical mechanism for modeling the dark zones of solid propellants.[20] The mechanism was developed for mixtures of $H_2/H_2O/CO/CO_2/NO/N_2/N_2O/HCN$ at temperatures between ~1000 and ~3000 K. It is based on the mechanism of Miller and Bowman[2] for modeling of nitrogen chemistry in combustion. Modifications include updated rate coefficient values, thermodynamics, and additional reactions. Reverses of all reactions are automatically included via calculation of equilibrium constants from thermodynamic data. Ar was readily added. For the present purposes, removal of C atom species has allowed reduction to ~110 reactions. The full mechanism is too long to present. However, the subset of reactions involving only nitrogen- and oxygen-containing species is presented in the companion paper.[6] Furthermore, sensitivity and rate analysis of the results show that, for conditions of the present experiments, only a few of the reactions have much significance. These reactions are shown in Table 2. Additional comments regarding our recent development of the subset of reactions used for modeling of H_2/N_2O and $H_2/N_2O/NH_3$ flames may be found in ref 24. The SENKIN time-dependent, homogeneous chemical reactor code[25] was utilized for the calculations. Temperature and pressure were assumed constant. Implicit assumptions made in the application of this model are that mixing at the inlet is instantaneous and plug flow is appropriate for the reactor; that is, diffusion is ignored. Possible effects of these assumptions are discussed later.

Prior to modeling the experiments with hypothetical traces of H_2O contaminant present, a few cases representative of the typical conditions (see Table 1) were modeled without H_2O added to the initial mixture. Most of the modeling was performed with a "standard" mixture of 0.001 77 mole fraction N_2O and 0.000 004 4 mole fraction O_2, the remainder being Ar, and pressure 405 mbar, which is representative of experimental conditions. It was found that the modeling of [O] must be done utilizing a two-step calculation, representing thermal reaction followed by photolysis. This holds true whether H_2O is included in the initial mixtures or not. The calculation is illustrated in Figure 2. The k_1 and k_2 expressions used are the final recommendations made in the following paper in this issue;[6] at 1076 K, these yield k_{tot} equal to that of the present measurements. The first step of the calculation represents the thermal decomposition of a minute fraction of the N_2O in the hot test mixture as it travels convectively through the reactor tube between the injection point and the photolysis/probe volume. This results in formation of a constant, trace, steady-state [O], hereafter referred to as $[O]_{SS}$.

The observation of a steady-state [O], 5×10^{-7} mole fraction in Figure 2, is caused by the formation of O atoms in reaction R3 and their destruction in reactions R1 and R2 (see Table 2). Assuming only reactions R1, R2, and R3 have appreciable rates and $[N_2O]$ is nearly constant, the resulting differential equation for [O] can be solved analytically. The general solution is

$$[O] = k_{3,uni}/k_{tot} + C \exp(-k_{ps1}t) \qquad (7)$$

where $k_{3,uni}$ is the apparent unimolecular rate coefficient of reaction R3 taking falloff into account and C is a constant of the integration to be determined using the proper $[O]_o$, the initial [O]. $k_{3,uni}/k_{tot}$ is recognized as the $[O]_{SS}$. The criterion for the $[O]_{SS}$ to be observed is $k_{tot}[N_2O] \gg k_{3,uni}$. This inequality is fulfilled over the range of conditions utilized in the experiments. Using eq 7 and the proper initial conditions, it is readily shown that the asymptotic approach of [O] to $[O]_{SS}$ after the injection of N_2O into the reactor exhibits a $[1 - \exp(-k_{ps1}t)]$ dependence, while the [O] decays after photolysis have an exponential form similar to eq 6. The exponential forms for each have the same pseudo-first-order rate coefficient, k_{ps1}, as may be observed in

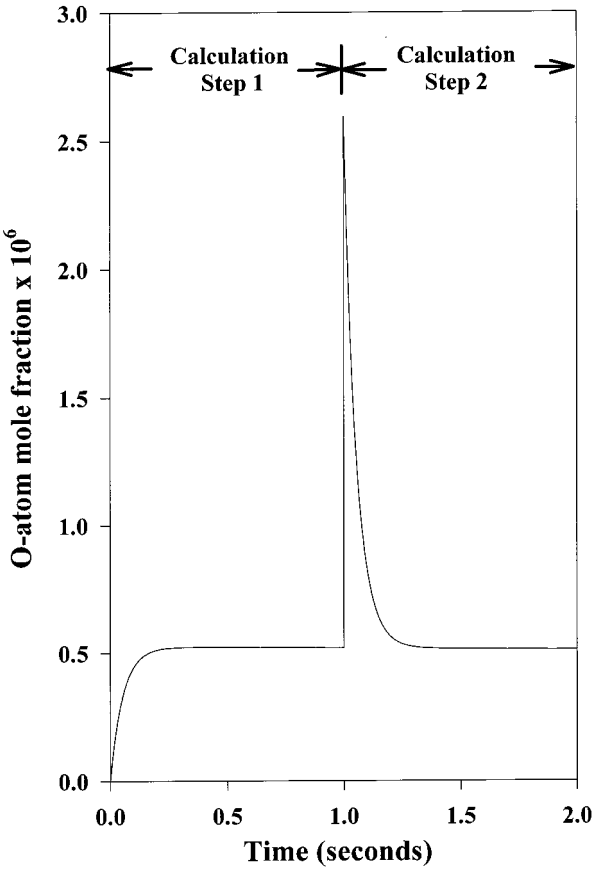

Figure 2. O atom profile for an example modeling run. The example used the standard mixture (no H_2O present) and pressure described in the text, and $T = 1076$ K. The k_{tot} value used is taken from ref 6. The portion from 0 to 1.0 s, a typical residence time, indicates exponential [O] increase to a constant, steady-state level due to thermal reaction of a small fraction of the N_2O during that period. Photolysis was assumed to occur at 1.0 s. The exponential decay after photolysis represents the experimentally measured quantity.

Figure 2. These curious characteristics result from decomposition producing the reactant radical and would occur in other, similar cases. Because the $[O]_{SS}$ is constant, its presence does *not* adversely affect the extraction of k_{ps1} via fits to eq 6. The value of the $[O]_{SS}$ formed during the thermal reaction phase, and to which [O] decays after the photolysis, is independent of $[N_2O]$ as long as an appreciable $[N_2O]$ is present. Following these predictions, experiments have shown, by observing background variation vs reactor temperature, that the $[O]_{SS}$ can contribute substantially to the background constant, *B*, in eq 6.

The concentrations of *all* species *except* O atoms at the end of the thermal reaction step are then used as initial conditions for the second, photolysis step of the calculation. The calculations indicate that if the thermal reaction step is ignored and the modeling is initiated with an assumed [O] formed by photolysis smaller than that found at the steady state, then the [O] is predicted to *increase* to the $[O]_{SS}$ after the photolysis pulse. Growth in [O] after the pulse contradicts the experimental observations, proving the necessity of the thermal decomposition calculations.

For the photolysis step, the initial [O] is increased above the $[O]_{SS}$, and the calculation is reinitiated. The [O] then decays back to the baseline $[O]_{SS}$ (see Figure 2). Fits of the simulated decays to eq 6 are excellent. These fitted k_{ps1} values almost exactly reflect the assumed values of k_{tot} and initial $[N_2O]$, as expected, at the lowest temperatures used. However, possible deviations were predicted due to contributions from significant N_2O decomposition at the higher temperatures. Because this decomposition leads to NO and NO_2 formation, the −R7 and R8 reaction sequence may be important at the highest temperatures utilized (−R7 indicates the reverse of reaction R7). The consequences will be discussed later.

When hypothetical traces of H_2O were added to the modeling mixtures, both [O] and [OH] during the thermal decomposition step increase to nearly constant plateau levels after a small fraction of the residence time. Between the inlet tube and the photolysis zone, the [OH] builds to a trace value due to $N_2O + M \rightarrow N_2 + O + M$ (R3) and $O + H_2O \rightarrow OH + OH$ (−R6). After the photolysis pulse, in addition to reactions R1−R3, the reactions $H + N_2O \rightarrow OH + N_2$ (R4) and $O + OH \rightarrow O_2 + H$ (−R5) are predicted to have the largest effects, accelerating the O atom decays. Note that reaction R4 combined with reaction −R5 represents a cycle catalyzed by H and OH. Therefore, even though only small traces of H and OH could be present, these species would not be consumed during the [O] decrease. This fact explains why the effects of even a few parts per million H_2O as a contaminant could significantly alter the resulting apparent rate coefficient.

For the present experimental conditions, modeling indicates H_2O would increase both the rates of [O] growth to constant $[O]_{SS}$ levels during the thermal decomposition step and the decay rates to these levels in the photolysis step by equal amounts. Plots of the predicted [O] decreases with $[H_2O]$ in the mixtures appeared to be exponential upon visual examination. However, fits of these decays to eq 6 revealed such mixtures would actually produce small deviations from exponential behavior. For example, the differences between predicted [O] decreases and exponential fits were about 5% relative to $[O]_o - [O]_{SS}$ for 5−20 ppm H_2O.

Parametric studies of the fitted decays have revealed two additional features of the chemical system. These features would complicate detection of the effects of H_2O. First, the predicted order of the rate in $[N_2O]$ is fairly close to unity, for the range of $[N_2O]$ used in the experiments, if all other variables are held constant. Second, the order in $[H_2O]$ is much less than unity (0.33 at 1076 K; 0.4 at 1276 K). These characteristics make ruling out possible systematic errors due to the presence of H_2O nontrivial because (1) small deviations from exponential behavior are difficult to see in real data with noise and (2) the $[N_2O]$ order being near unity means plots of predicted k_{ps1} vs $[N_2O]$ exhibit approximately linear behavior despite the assumed $[H_2O]$. Also, the standard procedure followed in the experiments to reveal the presence of contaminants or impurities is to widely vary reactant and carrier gas partial pressures. Were a contaminant present, this procedure would yield differing reactant-to-contaminant ratios. It is expected that varying these ratios will reveal the presence of appreciable contaminant effects because extracted rate coefficients will exhibit systematic trends. However, since the predicted order in $[H_2O]$ is small, the effect of varying H_2O contaminant-to-reactant ratios would not be as large as one expects for a contaminant of higher reaction order.

An example of a predicted [O] decrease with significant $[H_2O]$ present is shown in Figure 3, upper panel. In this example, the standard mixture with 5 ppm H_2O added was used with the standard pressure and an assumed temperature of 1076 K. The HS85 k_1 and k_2 expressions were used. Also shown in Figure 3, upper panel, is a least-squares fit of the exponential function of eq 6 to the simulated decay curve, the time intervals in the latter having been first interpolated to match the data sampling rate of the experiment. As can be seen, although the predicted decay curve looks nearly exponential, the exponential fit is not

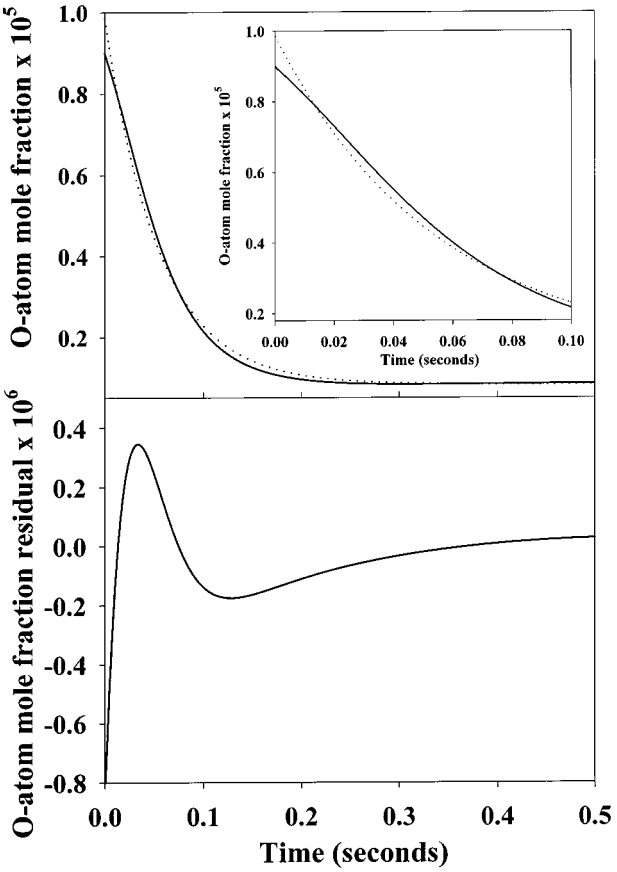

Figure 3. Predicted O atom decay curve (upper panel) and residual plot (lower panel) with H_2O as a hypothetical contaminant at 5 ppm. In the upper panel, the solid line represents the [O] profile, while the dotted line shows the least-squares fit to an exponential function, eq 6, for the oxygen atom decay. An enlargement of the early-time [O] curve is presented in the inset in the upper panel, revealing the deviation from exponential behavior. k_1 and k_2 from HS85[7] were used. The assumed conditions were identical to those in Figure 2.

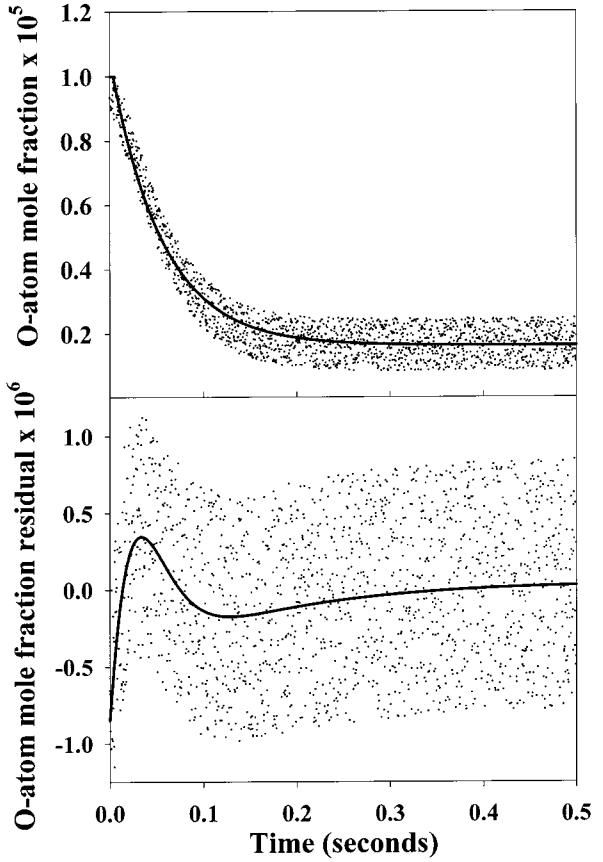

Figure 4. Predicted O atom decay curve with random noise added (upper panel) and corresponding residuals plot (lower panel). Assumed conditions are the same as for Figure 3, except that noise has been added to simulate a *S*/Sc (signal-to-scatter ratio) of 5. The solid line in the upper panel is the fit of the simulated data points to eq 6. The noise-free residuals plot from Figure 3, lower panel, is repeated as the solid curve in the lower panel here to demonstrate that the scatter envelope is centered about the noise-free plot, as expected.

perfect; the differences are undoubtedly *very* much larger than the numerical error of the SENKIN code. At short times, the exponential fit is slightly higher than the predicted "experimental" decay curve, crosses it at 0.014, 0.075, and 0.373 s, and finally approaches the same baseline asymptotically at long times. A plot of the residuals[16] of the fitting procedure is shown in Figure 3, lower panel. If the predicted curve were exponential, the residuals would be zero at all times. However, the residuals plot has a strange shape, reflective of the slight difference from exponential decay shown in the upper panel, with zeros at the points where the upper panel curves cross.

The following question naturally arises: If the HS85 recommended rate coefficients were correct, and if enough H_2O had been present in the current experiments to account for the measured decays, would the experimental data reduction procedures have revealed the deviation from exponentiality and led to rejection of the data? To answer this question, simulated decay curves were prepared. Enough constant-level white noise was added, using a random number generator, to mimic the *S*/Sc ratios observed in typical experiments. Here, *S*/Sc is defined as the signal-to-scatter ratio, where *S* is equivalent to I_o, and Sc is the full width of scatter at the baseline. One such curve, with exponential fit, is shown in Figure 4, upper panel. The curve has $S/Sc \cong 5$; larger *S*/Sc values were achieved in most of the actual experiments. The corresponding residuals plot is shown in Figure 4, lower panel, which demonstrates that the band of residuals from noisy "data" is centered about the noise-free plot as one would expect. The unusual departures at short times from the expected band centered about zero would have been detected even by visual inspection during data reduction, if present in the actual experiments.

The simulated case in Figure 4, upper panel, with $S/Sc = 5$ and $Z = -1.28$ shows that such a low *S*/Sc would not cause the runs test to lead to data rejection. However, the unusual shape of the residuals plot shown in the lower panel would be the basis for rejection of the data using the visual inspection method. A similar example was tested with $S/Sc = 10$, which resulted in $Z = -2.25$ and an even more unusual residuals plot; the result is rejection of the data by either method. The nonexponentiality of the simulated [O] decreases in the presence of 5 ppm H_2O becomes more obvious as the *S*/Sc ratio increases. In the experiments, attempts to increase *S*/Sc by averaging results from more photolysis flashes would have been made in such a case. However, such efforts could only have resulted in an increased awareness of the nonexponentiality of the decays. Many of the experimental decays have $S/Sc \geq 10$. *All the experimental [O] decays, such as in Figure 1 with* $S/Sc \approx 6$*, pass both tests of exponentiality, thus yielding strong evidence that [*H_2O*] cannot be as high as 5 ppm in the actual experiments.*

IV. Results

The determinations of k_{tot} are summarized in Table 1. The experimental parameters *P*, total pressure; [M], the total gas

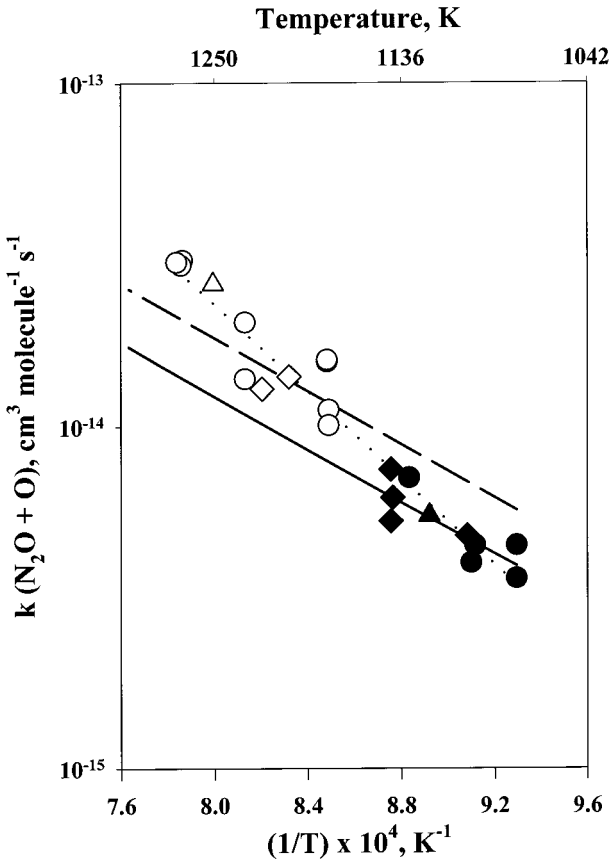

Figure 5. Arrhenius plot of measured data points for k_{tot}. The solid symbols represent retained data, while the open symbols represent data rejected from the final fit for recommended rate coefficients. Key: ····· least-squares fit to the present measurements; ——— recommendation from Ref. 6, fit to retained literature data using only the present 10 lowest-temperature data points; — — fit to retained literature data including all present measurements; ○, ● the O atom source was SO_2 laser photolysis; ◇, ◆ the O atom source was SO_2 flash-lamp photolysis; △, ▲ the O atom source was O_2 flash-lamp photolysis.

concentration; *z*, the distance from the top of the cooled inlet to the center of the reaction zone; $\bar{v}$, the average linear gas velocity; [photolyte], the concentration of the O atom precursor; and *F*, the energy of the laser or the flash lamp, were varied over wide ranges. To demonstrate that the rate coefficients do not depend on any of these parameters, plots of $[k(T) - k_i]/k(T)$ vs these parameters were made (not shown), where $k(T)$ represents the rate coefficients obtained from the fit expression given below and k_i are the individual k_{tot} rate coefficients measured. These residuals plots are independent of these parameters. To avoid systematic errors due to the nature of the O atom precursor or the photolysis source, two precursors (SO_2 or O_2) and laser photolysis or flash photolysis were used. No dependence on these factors is found, either. Below 1076 K the reaction became too slow for accurate measurements. Attempts at measuring k_{tot} at temperatures above 1276 K exhibited increasing scatter and a dependence on residence times, indicating significant decomposition of the N_2O. These measurements were disregarded.

Figure 5 shows the present data fitted to the form $A \exp(-E_a/RT)$ where $\pm\sigma_{k_i}$ and $\pm\sigma_T/T = 2\%$ contribute to the weighting of each point. The fitted expression is

$$k_{tot}(1075-1275\ \mathrm{K}) = 2.7 \times 10^{-9} \exp(-14580K/T)\ \mathrm{cm^3\ molecule^{-1}\ s^{-1}} \quad (8)$$

The variances and covariance are $\sigma_A^2 = 1.02\ \mathrm{A}^2$, $\sigma_E^2 = 1.41 \times 10^6$, and $\sigma_{AE} = 1.2 \times 10^3$ A. The variances and covariance are combined by the method of Wentworth,[26] which yields a precision at the 2σ level of ±12% to ±22%, depending upon temperature. Allowing ±20% for any unrecognized systematic errors then leads to a 2σ accuracy level of ±29%.

In modeling the present experiments, computations for the highest temperatures used predict that during its travel down the reactor tube a substantial portion of the N_2O could decompose, producing, among other species, N_2, NO, and NO_2. Predictions indicate formation of NO and NO_2 could substantially increase the observed rate of O atom decay by catalysis via the −R7 and R8 reaction sequence. Simulation indicates that if this were to occur, the [O] decays would still be closely exponential; pseudo-first-order kinetics are obtained because [N_2O], [NO], and [NO_2] are nearly constant on the time scale of the decays. However, the situation is complicated because this effect would be compensated by a decrease in the decay rate due to a substantial decomposition of the N_2O. The situation is too sensitive to key rate parameters for reliable quantitative prediction and, indeed, even to be sure whether the measured k_{tot} values would be low or high. Calculations indicate the N_2O decomposition and NO/NO_2 catalytic effect are altogether negligible at the lower temperatures used. However, it cannot be accurately assessed at what temperature these effects become important. At high enough temperatures, reactant decomposition generally results in a large amount of scatter in measured rate coefficients; this is what was observed above 1280 K. Although there does appear to be slightly higher scatter in the 1178−1276 K portion of the data, the difference vs scatter at the lower temperatures is not large. In addition, the predicted temperature at which N_2O decomposition becomes important might be ∼50−100 K different from experimental observations for several reasons: (1) the amount of decomposition predicted depends strongly on assumed rate coefficients and their uncertainty limits, especially k_3, (2) during the first few centimeters of travel through the tube past the injection point, the N_2O must mix with hot gases and reach thermal equilibrium before much reaction commences, and (3) during travel through the tube, reactant gases come into contact with the wall; for O-atoms, this results in a constant, diffusion-related loss (wall recombination), reducing the background $[O]_{SS}$ discussed in the previous section. There is no simple way to include these effects in the modeling. Since the rate constant for loss due to diffusion is essentially constant as [N_2O] is varied, it does not affect the reliability of the predictions. Therefore, diffusion was ignored in the computations. However, the effect could reduce the amount of N_2O decomposition in the experiments, as compared to the model, because the $[O]_{SS}$ and, hence, the rates of reactions R1 and R2 are reduced.

Since the 1178−1276 K data have survived the exponentiality tests and do not exhibit great scatter, they have been presented in Table 1. Nevertheless, there is slightly larger scatter in that temperature range as opposed to the lower temperature portion of the data. Also, there appears to be a trend toward slightly larger *Z* values in the higher temperature portion of the data set (not shown), though the values meet standards normally used ($|Z| \leq 1.5$). When all 22 of the present data points are included in the fit to obtain recommendations for k_1 and k_2 expressions (the present data set plus nine from the literature; see ref 6), a skewing of the slope of k_{tot} from the overall fit vs the trend of

the present full data set results, Figure 5. A linear fit of the 12 highest temperature points has a suspiciously high A factor of 1×10^{-9} cm^3 molecule^{-1} s^{-1}, as does the fit to all 22 points, eq 8. Further, this 12-point fit has a slope about 1.4 times that of the 10 lowest temperature points. This slope change seems large for such a short temperature range. These observations may be indicative of an underlying systematic effect. These considerations, coupled with the modeling prediction that decomposition likely increases k_{tot} values toward the high-temperature end of the data set, have led us to retain only the lower temperature portion of the data in the fit for recommended values. As can be seen in Figure 5, when only that portion is used, the overall fit passes through those 10 points with excellent agreement in slope. Fitting those 10 points at lowest temperatures alone, the recommended result of the present work is

$$k_{tot}(1075-1140\ \mathrm{K}) = 3.2 \times 10^{-11} \exp(-9686K/T)\ \mathrm{cm}^3\ \mathrm{molecule}^{-1}\ \mathrm{s}^{-1} \quad (9)$$

(not shown). The corresponding 2σ precision and accuracy limits are ±12% and ±26%, respectively.

V. Discussion

The assumption of 5−10 ppm H_2O used for much of the modeling in section III is of special interest. A 5 ppm concentration is required at the highest temperatures and 10 ppm at the lowest temperatures used in the experiments to explain the observations if the HS85 rate coefficient expressions were correct and conjectural H_2O contamination caused the fast observed [O] decreases. The computed decay in Figure 2, which was obtained with k_{tot} values equal to those measured in the present experiments at 1076 K and no H_2O in the modeling mixture, has a 0.037 s half-life, which is typical of the experiments. If instead the HS85 k_1 and k_2 values are used for the same conditions, the computed half-life is 0.134 s. Retaining the HS85 k values, but including 5 ppm H_2O in the initial mixture, as in Figure 3, upper panel, the half-life is 0.047 s. With 10 ppm H_2O and the HS85 k values, the half-life is 0.037 s (not shown). These results demonstrate the potentially large effect of H_2O as a contaminant. However, the modeling results also clearly indicate that if 5 ppm or more H_2O had been present, the experimental residual analysis procedures would have revealed an underlying problem. *Such is not the case, leading to the conclusion that the HS85 values are too small for the present temperature range.* Predictions were also made assuming concentrations of H_2O less than 5 ppm. At $[H_2O] \leq 1.5$ ppm, it is uncertain whether the residuals analysis would have detected the nonexponentiality of the decays. However, as discussed in detail in the Experimental Section, the $[H_2O]$ could not have been higher than 0.2 ppm. This value is a very conservative estimate. Therefore, calculations were performed with and without 0.2 ppm H_2O in the initial mixture, using either the HS85 rate coefficients or those measured in the present work. The difference in decay rates caused by such a trace amount of H_2O is calculated to be only a few percent, which is negligible considering the experimental tolerances. *Thus, it has been shown on the basis of two lines of reasoning that H_2O contamination in the experiments cannot account for the difference between the present rate coefficients and the smaller ones from previous recommendations.*

In Figure 6, the present retained data are compared to other results of interest. First, consider the HS85 recommendation[7] and the DDCH92 result[9] for k_{tot} (obtained in each case by adding $k_1(T)$ and $k_2(T)$ expressions). Note both have been extrapolated to temperatures of the present study. The HTP data fall between the two earlier results. The present data agree with DDCH92 in that k_{tot} is much larger at low temperatures than had been thought previously (e.g., HS85). At the low-temperature end of the current data, the results are a factor of 5 larger than the HS85 recommendation, well outside tolerances (~50%) implied by a short extrapolation of the recommendation. They are a factor of 4 smaller than an extrapolation of the DDCH92 results. Considering the error limits in the k_1 and k_2 expressions from DDCH92, the present results are within tolerances of the extrapolation of the DDCH92 results, although such a long extrapolation is a suspect procedure.

The present data are further compared with recent data on the title reaction in Figure 6. The solid curve is the recommended $k_1(T) + k_2(T)$ from the following paper in this issue.[6] The high-temperature portion of this fit is in fair agreement with prior recommendations.[5,7,8,11] Also shown at high temperatures is the result for k_2 from DDCH92. As can be seen, at high temperatures, k_2 from DDCH92 is much smaller than k_{tot}; their measured k_1 and k_2 values indicate that k_1 (not shown) is considerably larger than k_2 above ~2050 K and that k_1 and k_2 are equal at ~2050 K. Their measurements on k_2 extended to a lower limit of 1940 K. At this temperature, because of the error limits in the reported expressions, one cannot conclude directly that $k_2 > k_1$. However, on the basis of their fitted expressions, the authors of DDCH92 suggested k_2 dominates below ~2050 K. Estimates for the k_1 expression of the critical review,[6] obtained using the retained measurements of k_1 from the literature prior to fitting, indicated the proper k_1 rate coefficients would be much smaller at the temperatures of the present study than the presently observed k_{tot} values. *Thus, the present experimental k_{tot} results, combined with the retained k_1 values,[6] yield the conclusion that $O_2 + N_2$ is the primary intermediate temperature product channel, confirming the DDCH92 suggestion.*

Also shown in Figure 6 are the results of earlier intermediate temperature measurements. The recent upper limit k_{tot} values from Ross et al.[27] disagree rather strongly with the present results. Their upper limit data points result from complex modeling of shock tube experiments designed primarily to obtain rate coefficients for $N_2O + M$. It is theoretically difficult to reconcile such small intermediate temperature rate coefficient values with the well-established, near-linear region of the high-temperature results (about 1675−4080 K), whether the notion is accepted that reaction R1 dominates at high temperature or not. A fit of the high-temperature data together with the ref 27 data would produce a k_{tot} Arrhenius plot with a very pronounced downward curvature. On the other hand, an Arrhenius plot with upward curvature, such as the recommendation from the companion paper[6] shown in Figure 6, is easily explained by the occurrence of the two reaction channels.[6] Additionally, k_1 could be inferred via studies on the reverse reaction at intermediate temperatures as low as 1370 K, as discussed in detail in ref 6. These rate coefficient measurements survived critical tests and are used in the overall fit for recommended expressions. The intermediate temperature rate coefficients agree well with the high-temperature data for k_1. The k_1 expression from these studies of the reverse reaction is much larger at intermediate temperatures than the results of ref 27 would indicate. Thus, the ref 27 results disagree with not only the data presented herein but all pertinent prior results.

Qualitative support for the notion that reaction R2 dominates the reaction at intermediate temperatures, and that k_{tot} is larger than most prior works indicate, is provided by preliminary results of Lin and Tsay[28] for k_2 (see Figure 6). Comparison of

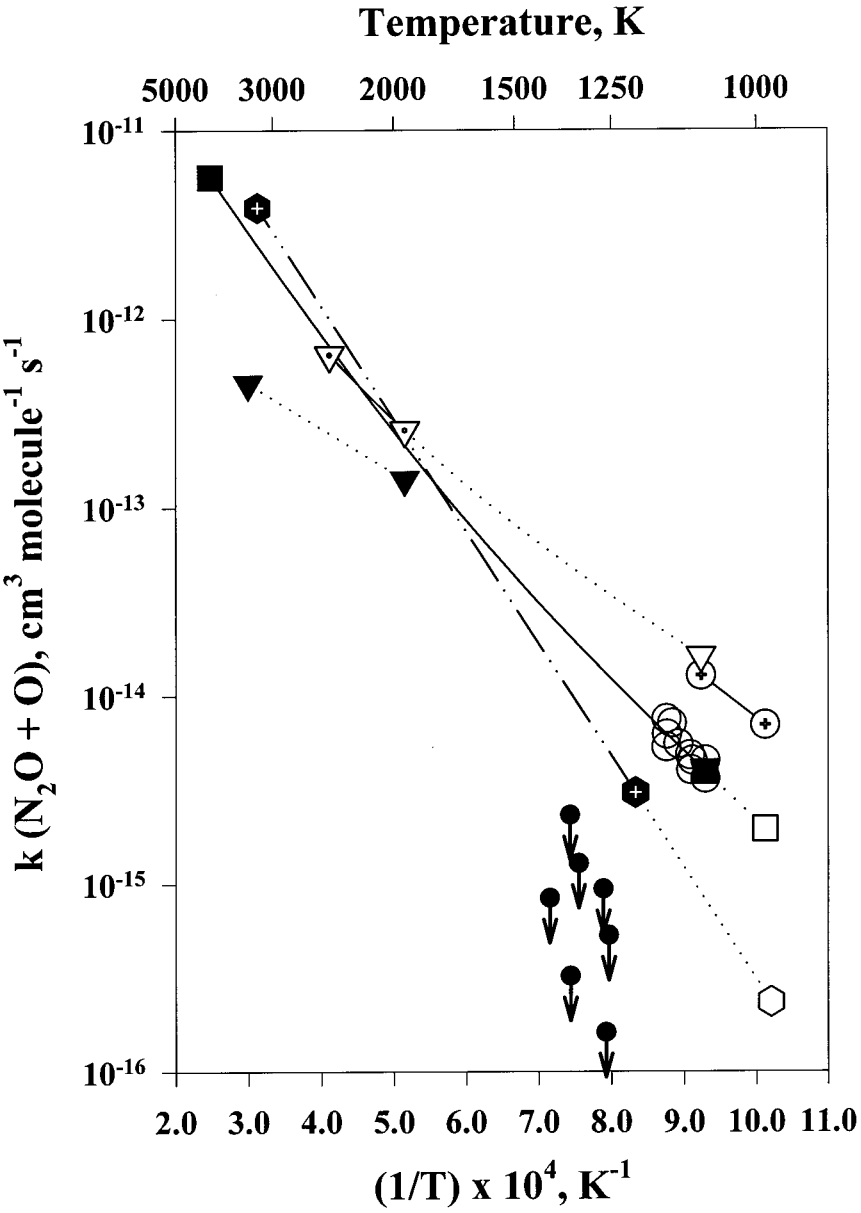

Figure 6. Arrhenius plot comparing the present results to prior works. Extrapolation beyond the recommended temperature range for a particular rate expression is denoted by a dotted line with a hollow symbol at the end. Key: ▼·····▼ DDCH92[9] k_2 result; ■——■ recommendation for k_{tot} from ref 6; ▽——▽ DDCH92[9] k_{tot} result; ⊕···⊕ HS85[7] k_{tot} recommendation; ⊙——⊙ k_2 from Lin and Tsay,[28] ↓ upper limit values for k_{tot} from Ross et al;[27] ○ present experimental data.

the present k_{tot} values directly to k_2 from Lin and Tsay is reasonable because the companion paper[6] concludes that k_1 only contributes ~10% to k_{tot} at the present temperatures. The Lin and Tsay experiments utilized a static reactor with mixtures of N_2O/Ar. Complex modeling was necessary to extract the rate coefficients. Their result agrees well with an extrapolation of the DDCH92 results for k_2 (or k_{tot}); it is larger than the present direct measurements indicate. Note, though, that the slope of Lin et al.'s k_2 agrees quite well with the present results for k_{tot}. Exact conditions and error limits for their results were not available at the time of writing of this paper.

VI. Conclusions

The first measurements on the title reaction performed under conditions in which it is well isolated from the effects of other reactions, i.e., complex chemical modeling was *not* required to obtain the result, were reported. The data, combined with other works, support the suggestion of a recent high-temperature shock tube study, DDCH92,[9] that the two product channels do not have equal rate coefficient expressions, as previously thought. Rather, the O_2 + N_2 channel dominates at intermediate temperatures. The new data provide a much more precise intermediate temperature determination of the total rate coefficients of the O + N_2O reaction than can be obtained by extrapolation of high-temperature results. In the companion paper,[6] the HTP data are considered along with earlier studies, and recommended rate coefficients for the two channels are presented.

Acknowledgment. The work at RPI was supported by ARO under Grants DAAH04-95-1-0098 and DAAG55-98-1-0183. We thank W. F. Flaherty for his valuable technical assistance and M. Leanovich for his help with some of the measurements.

References and Notes

(1) (a) Fifer, R. A. In *Fundamentals of Solid-Propellant Combustion*; Kuo, K. K., Summerfield, M., Eds.; Progress in Astronautics and Aeronautics, Vol. 90, American Institute of Aeronautics and Astronautics: New York, 1984; Chapter 4. (b) Melius, C. F. In *Chemistry and Physics of Energetic Materials*; Bulusu, S. N., Ed.; Kluwer: Dordrecht, The Netherlands, 1990; Chapter 4.

(2) Miller, J. A.; Bowman, C. T. *Prog. Energy Combust. Sci.* **1989**, *15*, 287.

(3) Dove, J. E.; Nip, W. S.; Teitelbaum, H. *Fifteenth Symposium (International) on Combustion*; The Combustion Institute: Pittsburgh, 1975; p 903.

(4) Troe, J.; Wagner, H. Gg. In *Physical Chemistry of Fast Reactions*; Levitt, B. P., Ed.; Plenum: London, 1973; Chapter 1.

(5) Baulch, D. L.; Drysdale, D. D.; Horne, D. G. *Evaluated Kinetics Data for High-Temperature Reactions. Vol. 2. Homogeneous Gas-Phase Reactions of the H_2-N_2-O_2 System*; Butterworths: London, 1973.

(6) Meagher, N. E.; Anderson, W. R. *J. Phys. Chem. A* **2000**, *104*, 6013.

(7) Hanson, R. K.; Salimian, S. In *Combustion Chemistry*; Gardiner, W. C., Ed.; Springer: New York, 1985; Chapter 6.

(8) Tsang, W.; Herron, J. T. *J. Phys. Chem. Ref. Data* **1991**, *20*, 609.

(9) Davidson, D. F.; DiRosa, M. D.; Chang, A. Y.; Hanson, R. K. In *Shock Waves*; Takayama, K., Ed.; Springer: Berlin, 1992; Vol. 2, p 813.

(10) Allen, M. T.; Yetter, R. A.; Dryer, F. L. *Combust. Flame* **1997**, *109*, 449.

(11) Dean, A. M.; Bozzelli, J. W. Combustion Chemistry of Nitrogen. In *Gas-Phase Combustion Chemistry*; Gardiner, W. C., Jr., Ed.; Springer-Verlag: New York, 2000; Chapter 2.

(12) Zuev, A. P.; Starikovskii, A. Y. *Khim. Fiz.* **1991**, *10*, 179; *Sov. J. Chem. Phys.* (*Engl. Transl.*) **1992**, *10*, 255.

(13) Ko, T.; Marshall, P.; Fontijn, A. *J. Phys. Chem.* **1990**, *94*, 1401.

(14) Marshall, P.; Ko, T.; Fontijn, A. *J. Phys. Chem.* **1989**, *93*, 1922.

(15) Marshall, P. *Comput. Chem.* **1987**, *11*, 219.

(16) Ko, T.; Adusei, G. Y.; Fontijn, A. *J. Phys. Chem.* **1991**, *95*, 8745.

(17) Draper, N. R.; Smith, H. *Applied Regression Analysis*; Wiley: New York, 1981; Chapter 3.

(18) Johnsson, J. E.; Glarborg, P.; Dam-Johansen, K. *Twenty-Fourth Symposium (International) on Combustion*; The Combustion Institute: Pittsburgh, 1992; p 917.

(19) Allen, M. T.; Yetter, R. A.; Dryer, F. L. *Int. J. Chem. Kinet.* **1995**, *27*, 883.

(20) (a) Anderson, W. R.; Ilincic, N.; Meagher, N. E.; Seshadri, K.; Vanderhoff, J. A. *32nd JANNAF Combustion Subcommittee Meeting and 1995 Propulsion Systems Hazards Subcommittee Meeting, Joint Sessions*; CPIA Publication 638; 1995; Vol. 1, p 197. (b) Anderson, W. R.; Meagher, N. E.; Ilincic, N.; Seshadri, K.; Vanderhoff, J. A. Manuscript in preparation.

(21) Röhrig, M.; Petersen, E. L.; Davidson, D. F.; Hanson, R. K. *Int. J. Chem. Kinet.* **1996**, *28*, 599.

(22) Glarborg, P.; Johnsson, J. E.; Dam-Johansen, K. *Combust. Flame* **1994**, *99*, 523.

(23) Masten, D. A.; Hanson, R. K.; Bowman, C. T. *J. Phys. Chem.* **1990**, *94*, 7119.

(24) (a) Sausa, R. C.; Anderson, W. R.; Dayton, D. C.; Faust, C. M.; Howard, S. L. *Combust. Flame* **1993**, *94*, 407. (b) Dayton, D. C.; Faust, C. M.; Anderson, W. R.; Sausa, R. C. *Combust. Flame* **1994**, *99*, 323. (c) Sausa, R. C.; Singh, G.; Lemire, G. W.; Anderson, W. R. *Twenty-Sixth Symposium (International) on Combustion*; The Combustion Institute: Pittsburgh, 1996; p 1043.

(25) Lutz, A. E.; Kee, R. J.; Miller, J. A. Sandia National Laboratories Technical Report SAND87-8248; October 1988.

(26) Wentworth, W. E. *J. Chem. Educ.* **1965**, *42*, 96, 162.

(27) Ross, S. K.; Sutherland, J. W.; Kuo, S. C.; Klemm, R. B. *J. Phys. Chem. A* **1997**, *101*, 1104.

(28) (a) Lin, M. C. Private communication. (b) Tsay, T. S. Master's Thesis, Emory University, 1994.